

Magnetic coupling in EE and EO azido-bridged binuclear copper complexes: Synthesis, structure and magnetic studies

Ishita Banerjee^a, Jaromir Marek^b, Radovan Herchel^c, Mohammad Ali^{a,*}

^a Department of Chemistry, Jadavpur University, Kolkata 700 032, India

^b Laboratory of Functional Genomics and Proteomics, Institute of Experimental Biology, Faculty of Science, Masaryk University, Kamenice 5/A2, CZ-625 00 Brno, Czech Republic

^c Department of Inorganic Chemistry, Faculty of Science, Palacky University, Tr. 17, Listopadu 12, CZ-771 46 Olomouc, Czech Republic

ARTICLE INFO

Article history:

Received 4 August 2009

Accepted 15 December 2009

Available online 14 January 2010

Keywords:

EE and EO bridging

Synthesis

Crystal structures

Ferro and antiferromagnetic coupling

ABSTRACT

Four azide bridged dinuclear copper(II) complexes, $[\text{Cu}_2(\text{L}^{\text{X}})_2(\text{N}_3)_2](\text{ClO}_4)_2$, with L^{X} = substituted *N,N*-bis[(3,5-dimethylpyrazole-1-yl)-methyl]benzylamine, $[\text{X} = \text{H}$ (**1**), OMe (**2**), Me (**3**) and Cl (**4**)] have been synthesized, out of which complexes **1** and **2** have been characterized structurally. In Complex **1** the two bridging azide ligands have connected the two metal centers in an end-on (**EO**) fashion with αSP (asymmetric Square Pyramidal) geometry and showed a weak antiferromagnetic interaction ($J = -3.34 \text{ cm}^{-1}$). On the contrary, in complex **2**, the two metal centers have been connected in end-to-end (**EE**) fashion exhibiting moderately strong ferromagnetic interaction ($J = +19.7 \text{ cm}^{-1}$). Cyclic voltammetric studies performed on all the four complexes show a reasonably good correlations when $E_{1/2}$ for $\text{Cu}^{\text{II}}\text{Cu}^{\text{II}} \rightarrow \text{Cu}^{\text{II}}\text{Cu}^{\text{III}}$ and $\text{Cu}^{\text{II}}\text{Cu}^{\text{III}} \rightarrow \text{Cu}^{\text{III}}\text{Cu}^{\text{III}}$ oxidations are plotted against σ (substituent constants) with $\rho = -0.182$ ($R^2 = 0.92$) and -0.684 ($R^2 = 0.99$) respectively.

© 2009 Elsevier Ltd. All rights reserved.

1. Introduction

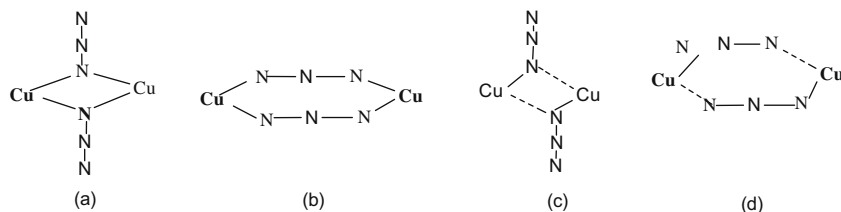
The development of the chemistry of binuclear metal complexes has been stimulated by a desire to synthesize model systems that may mimic the active sites of metallo-biomolecules [1–6], bind and activate small molecules [7–10] and be used to investigate the mutual influence of two metal centers in terms of cooperative effect on the electronic, magnetic and redox properties. One of the most appealing properties of binuclear transition metal complexes is the possible appearance of exchange interactions between the metal centers. A synthetic strategy that is generally applied to build such molecular architectures is to use pseudohalides as ligands [11–14], because they provide versatile coordination behavior and generates dimeric and multidimensional polymeric magnetic materials that facilitate ferro- and antiferromagnetic interactions among the metal centers [15–30]. Depending upon the steric and electronic demand of coligands, azide can serve as end-on (μ -1,1 or **EO**) or an end-to-end (μ -1,3 or **EE**) bridging ligand Chart 1. Such azido-bridged copper(II) complexes are of great interest for biologists and bio-inorganic chemists to investigate the structural and functional role of active sites in copper proteins [11,31], and also for physical inorganic chemists seeking to design new magnetic materials. Chart 1 displays different modes of bridging of azide ligand along with the geometry around the metal center, and also the

mode of cooperative magnetic interactions between the metal centers. From the magnetic point of view, an unusual range of magnetic behavior can be obtained as a function of coordination mode of the azide bridging group. In case of di-bridged complexes with one or more symmetric **EO** azido bridging, the interaction between the metal ions is strongly antiferromagnetic [32,11], but when it bridges asymmetrically, the interaction is weak to moderately strong ferromagnetic [33]. In contrast, with symmetric **EE** bridging the interaction is dominated to be ferromagnetic, while for asymmetric **EE** bridge with short and long $\text{Cu-N}_{\text{azide}}$ bonds, the interaction is either negligible or very weakly antiferromagnetic depending on the geometry which tends to be trigonal bipyramidal (TBP) or Square Pyramidal (SP), respectively [31]. The azido-bridged binuclear complexes provide a stringent test for any theoretical analysis of the exchange coupling [34].

Copper(II) complexes of multidentate heterocyclic amine ligands coordinated to metal centers have found extensive use to generate biological models that mimic proteins such as hemocyanin and tyrosinase [35], a Type-3 copper proteins with strong antiferromagnetically coupled copper(II) centers and therefore EPR silent in the oxidized state [36]. Although there are few reports on the copper complexes of pyrazole-based ligands, which are mostly mononuclear in nature [37–47], no report on the azido-bridged copper(II) complexes of such ligands are available in the literature. Here, we report four azide bridged dinuclear copper(II) complexes of the ligands L^{X} ($\text{X} = \text{Cl}, \text{H}, \text{Me}$ and OMe), two of them have been characterized structurally and magnetically.

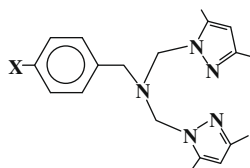
* Corresponding author. Tel.: +91 9433249716 (m); fax: +91 33 2414 6223.

E-mail addresses: m_ali2062@yahoo.com, mali@chemistry.jdvu.ac.in (M. Ali).



(a) : S (F), (b): S (AF), (c) AS (F), (d) AS (weak AF)

S = symmetric, AS = antisymmetric, F= Ferromagnetic and AF = antiferromagnetic

Chart 1. Different modes of bridging of azide ion to metal center and the nature of magnetic interactions.X = H(L^H), OMe(L^{OMe}), Me(L^{Me}) and Cl(L^{Cl})

2. Experimental

2.1. Materials and reagents

2.1.1. Synthesis of tripodal ligands

Preparation of 3,5-dimethyl pyrazole and (1-hydroxy methyl)-3,5-dimethyl pyrazole: 3,5-Dimethyl pyrazole and corresponding (1-hydroxy methyl)-3,5-dimethyl pyrazole have been prepared by following the literature procedures [48].

2.1.2. Preparation of ligands (L^X with X = Cl, H, Me and OMe)

All the ligands (L^X) were synthesized by following the literature procedure [48]. In a typical attempt, a solution of 12 mmol of respective substituted benzyl amines and 24 mmol of (1-hydroxy methyl)-3,5-dimethyl pyrazole in 50 ml acetonitrile was stirred

in a stoppered vessel at room temperature for 24 h. The water produced in the reaction was removed by drying over anhydrous Na₂SO₄. It was filtered and evaporated under reduced pressure. Oily substance thereby appeared was dissolved in diethylether and kept in refrigerator whereupon white crystalline product appeared was filtered and air dried in air.

L^{Cl}: Yield 55%. Calculated for Molecular formula: C₁₉H₂₄N₅Cl (357.5): C, 63.8; H, 6.71; N, 19.6; Found: C, 64.04; H, 6.49; N, 19.7%.

L^H: Yield 60%. Calculated for Molecular formula: C₁₉H₂₅N₅ (323.0): C, 70.5; H, 7.73; N, 21.67; Found: C, 70.62; H 7.76; N 21.5%.

L^{Me}: Yield 60%. Calculated value for Molecular formula: C₂₀H₂₇N₅ (337.0): C, 71.21; H, 8.01; N, 20.77; Found: C, 71.15; H 7.89; N 20.80.

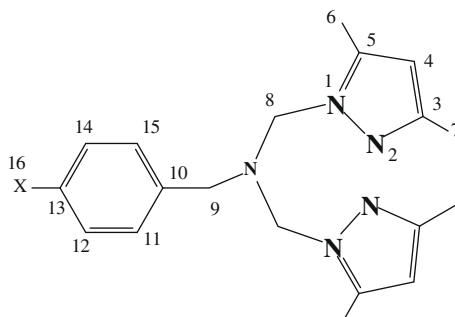
L^{OMe}: Yield 65%. Calculated value for Molecular formula: C₂₀H₂₇N₅O (353.0): C, 67.90; H, 7.64; N, 19.80; Found: C, 68.06; H 7.53; N 20.06.

Results of ¹H and ¹³C NMR studies on all the four ligands are listed in Table 1.

2.2. Preparation of azide bridged complexes

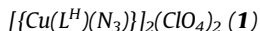
To a methanolic solution of 0.25 mmol of Cu(ClO₄)₂·6H₂O respective ligands were added. Immediately the colour of the solu-

Table 1
¹H and ¹³C NMR of ligand L^X.

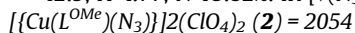


Ligand	¹ H NMR (CDCl ₃ , δ, ppm)	¹³ C NMR (CDCl ₃ , δ, ppm):
L ^{OMe} (X = OMe)	1.98 (6H,s); 2.19 (6H,s); 3.62 (2H,s); 3.76 (2H,s); 4.88 (4H,s); 5.77 (2H,s); 6.78–7.09 (4H,d)	147.52 (C3); 139.91(C5); 129.9 (C11,15); 127.9 (C10); 113.69 (C12,14); 105.64(C4); 64.74 (C8); 55.24(C16); 51.98(C9); 13.50 (C7); 10.67 (C6); 55.24 (C16, OMe)
L ^{Me} (X = Me)	1.99 (6H,s); 2.18 (6H,s); 3.63 (2H,s); 4.90 (4H,s); 5.77 (2H,s); 7.06 (4H,q)	147.52 (C3); 139.91 (C5); 136.78 (C13); 134.96 (C10); 128.98 (C11, 12, 14, 15); 105.63 (C4); 64.74 (C8); 52.22 (C9); 13.50 (C7); 10.67 (C6); 21.08 (C16, Me)
L ^H (X = H)	1.99 (6H,s); 2.17 (6H,s); 3.69 (2H,s); 4.93 (4H,s); 5.42 (2H,s); 7.1–7.3 (5H,m)	149.4 (C3); 140.9 (C5); 105.4 (C4); 127.3 (C13); 135.6 (C10); 128.5 (C11, 12, 14, 15); 61.4 (C8); 55.7 (C6); 18.0 (C7); 11.2 (C6)
L ^{Cl} (X = Cl)	2.32 (6H,s); 3.62 (1H,s); 4.80 (4H,s); 5.82 (2H,s); 7.78 (4H,s)	148.32 (C3); 139.92 (C5); 132.8 (C13); 129.9 (C11, 15); 128.02 (C12, C14); 106.04 (C4); 64.84 (C8); 55.24 (C6); 13.50 (C7); 11.2 (C6)

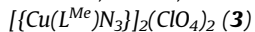
tion turned to blue, which on subsequent addition of 0.75 mmol of NaN_3 changed to deep green. It was stirred for further six hours whereupon the solution turned to brown. It was filtered and the filtrate was kept in refrigerator. Green crystals were formed. Complexes **1** and **2** yield single crystals on slow evaporation within couple of weeks. We failed to get suitable single crystals of complexes **3** and **4** even after several trials with different solvents.



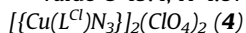
Yield 60%, Anal. Calc.: C 43.18, H 4.73, N 21.21%; Found: C 42.9, H 4.77, N 19.82%. IR [$\nu(\text{N}_3)$, cm^{-1}] = 2054.



Yield 70%, Anal. Calc.: C 43.0, H 4.83, N 20.07%; Found: C 42.83, H 4.80, N 19.98%. IR [$\nu(\text{N}_3)$] = 2055.



Yield 64%, Anal. Calc.: C 44.3, H 4.98, N 20.66%; Exptal. Calc. value C 45.4, H 4.87, N 20.2%. IR [$\nu(\text{N}_3)$] = 2038.



Yield 64%, Anal. Calc.: C 40.46, H 4.43, N 19.87%; Exptal. Calc. value C 40.6, H 4.80, N 19.9%. IR [$\nu(\text{N}_3)$] = 2073.

2.3. Physical measurements

Elemental analyses were carried out using a Perkin–Elmer 240 elemental analyzer. Infrared spectra (400–4000 cm^{-1}) were recorded from KBr pellets on a Nicolet Magna IR 750 series-II FT-IR spectrophotometers. ^1H and ^{13}C NMR were recorded in CDCl_3 on a Bruker 300 MHz NMR Spectrophotometer using tetramethylsilane ($\delta = 0$) as an internal standard. Electronic spectra were recorded on Agilent 8453 diode array UV–vis spectrophotometer. Electrochemical measurements were carried out using a computer-controlled AUTOLAB (model 263A VERSASTAT) electrochemical instrument with platinum tip as working electrode.

2.3.1. Crystal structure determination and structural refinement

Intensity data for complexes **1** and **2** were collected on a four-circle diffractometer Kuma KM-4 equipped with a CCD detector and an Oxford Cryostream Cooler (Oxford Cryosystems). The ω -scan technique with different κ and ϕ offsets for covering the whole independent part of reflections in the $2 < 2\theta < 25^\circ$ for monochromated (monochromator Enhance, Oxford Diffraction) Mo K α radiation ($\lambda = 0.71073 \text{ \AA}$) was performed. The data reductions were carried out using the CrysAlis RED (Oxford Diffraction) program. The cell parameters were refined from all strong reflections. We applied an empirical absorption correction as implemented in SCALE3 ABSPACK scaling algorithm (CrysAlis RED) on both datasets. The structures were determined by direct methods (SHELXS-97) and refined anisotropically on F^2 using full matrix least-squares procedure by SHELXL-97 [49]. Hydrogen atoms were included in the riding model approximation with C–H = 0.95, C–H₂ = 0.99, C–H₃ = 0.98 \AA . The final refinement details are given in Table 1.

3. Results and discussion

The IR peaks corresponding to $\nu(\mu-1,1$ or **EO**) or an end-to-end ($\mu-1,3$ or **EE**) appear in the range 2038–2073 cm^{-1} for all the complexes. This indicates that the N_3^- group bound to both the copper(II) center through its nitrogen atom, exhibiting an increase in its stretching frequency.

3.1. Structural description of $[\{\text{Cu}(\text{L}^{\text{H}})(\mu-1,1-\text{N}_3)\}_2(\text{ClO}_4)_2$ (**1**) (**EO**)

Complex **1** crystallizes from methanol as dark green solids. The details of structural determination for the compounds reported here are given in Table 2. Selected bond distances and bond angles

Table 2
Crystal data and details of the structure determination.

Formula	(1)	(2)
	$\text{C}_{38}\text{H}_{50}\text{Cu}_2\text{N}_{16}$, $2(\text{ClO}_4)$	$4(\text{C}_{40}\text{H}_{54}\text{Cu}_2\text{N}_{16}\text{O}_2)$, $8(\text{ClO}_4)$, O
Formula weight	1056.94	4483.97
Crystal system	Triclinic	Monoclinic
Space group	$P\bar{1}$ (No. 2)	$C2/c$ (No. 15)
<i>a</i> , <i>b</i> , <i>c</i> (\AA)	8.9889(6), 11.1947(6), 12.2791(7)	14.0929(4), 15.6767(6), 21.6474(10)
α , β , γ ($^\circ$)	74.740(5), 89.188(5), 70.984(5)	90, 91.966(3), 90
<i>V</i> (\AA^3)	1123.53(12)	4779.8(3)
<i>Z</i>	1	1
<i>D</i> (calc.) (g cm^{-3})	1.562	1.558
μ (Mo K α) (mm^{-1})	1.136	1.076
<i>F</i> (0 0 0)	546	2320
Crystal size (mm)	0.20 × 0.20 × 0.40	0.40 × 0.40 × 0.40
Temperature (K)	120	120
Radiation (\AA) Mo K α	0.71073	0.71073
θ Minimum–maximum ($^\circ$)	3.3, 25.0	3.2, 25.0
Dataset	–10;10; –13;11; –12;14	–16;16; –18;15; –25;23
Total unique data, <i>R</i> _{int}	7849, 3954, 0.013	16,202, 4227, 0.012
Observed data [<i>I</i> > 2 σ (<i>I</i>)]	3344	3943
<i>N</i> _{ref.} , <i>N</i> _{par}	3954, 302	4227, 351
<i>R</i> , <i>wR</i> ² , <i>S</i>	0.0238, 0.0664, 1.09	0.0310, 0.0743, 1.04
Maximum and average shift/error	0.00, 0.00	0.00, 0.00
Minimum and maximum resd. densities (e \AA^{-3})	–0.27, 0.35	–0.48, 0.55

$$w = 1/[\sigma^2(F_o^2) + (0.0700P)^2 + 1.5000P] \text{ where } P = (F_o^2 + 2F_c^2)/3.$$

Table 3
Selected bond distances (\AA) and bond angles ($^\circ$) for **1**^a and **2**^b.

1		2	
Cu1–N1	1.9798(17)	Cu1–N1	1.9656(17)
Cu1–N9	2.0802(16)	Cu1–N9	2.0755(17)
Cu1–N11	1.9715(17)	Cu1–N11	1.9743(19)
Cu1–N18	2.4272(16)	Cu1–N17	1.9593(19)
Cu1–N18_a	1.9619(17)	Cu1–N19_a	2.403(2)
N1–Cu1–N9	81.04(6)	N1–Cu1–N9	82.13(7)
N1–Cu1–N11	163.01(7)	N1–Cu1–N11	161.20(7)
N1–Cu1–N18	91.05(6)	N1–Cu1–N17	98.11(8)
N1–Cu1–N18_a	97.57(7)	N1–Cu1–N19_a	94.77(7)
N9–Cu1–N11	82.17(6)	N9–Cu1–N11	79.89(7)
N9–Cu1–N18	95.45(6)	N9–Cu1–N17	174.60(8)
N9–Cu1–N18_a	178.30(7)	N9–Cu1–N19_a	89.86(7)
N11–Cu1–N18	93.09(6)	N11–Cu1–N17	99.28(8)
N11–Cu1–N18_a	99.27(7)	N11–Cu1–N19_a	90.63(7)
N18–Cu1–N18_a	83.59(6)	N17–Cu1–N19_a	95.50(7)
Cu1_a–N18–N19	126.87(13)	Cu1_a–N19–N18	119.26(15)
Cu1–N18–N19	136.52(13)	Cu1–N17–N18	120.32(16)
Cu1–N18–Cu1_a	96.41(7)		

^a Symmetry $x + 1, -y + 1, -z + 1$.

^b Symmetry $-x + 1, y, -z + 3/2$.

for **1** are given in Table 3. The ORTEP diagram of cationic part of **1** is given in Fig. 1. There are one dimeric unit, $[\text{CuL}^{\text{H}}(\mu-\text{N}_3)_2]^{2+}$ with two equivalent (symmetry $x + 1, -y + 1, -z + 1$) copper atoms in the unit cell (Fig. 2) and two perchlorate anions just in *trans* disposition. The perchlorate ions are found to be normal though they are not coordinated to the metal centers. The center of one dimeric cation is located about a crystallographic center of inversion. Within a dimeric unit, the copper(II) centers are centro-symmetrically related and are bridged by azide ions in an asymmetric **EO** fashion. The copper(II) ion is coordinated to five nitrogens; three nitrogen atoms from the pyrazolyl-N and amin-N of L^{H} ($X = \text{H}$) and a nitro-

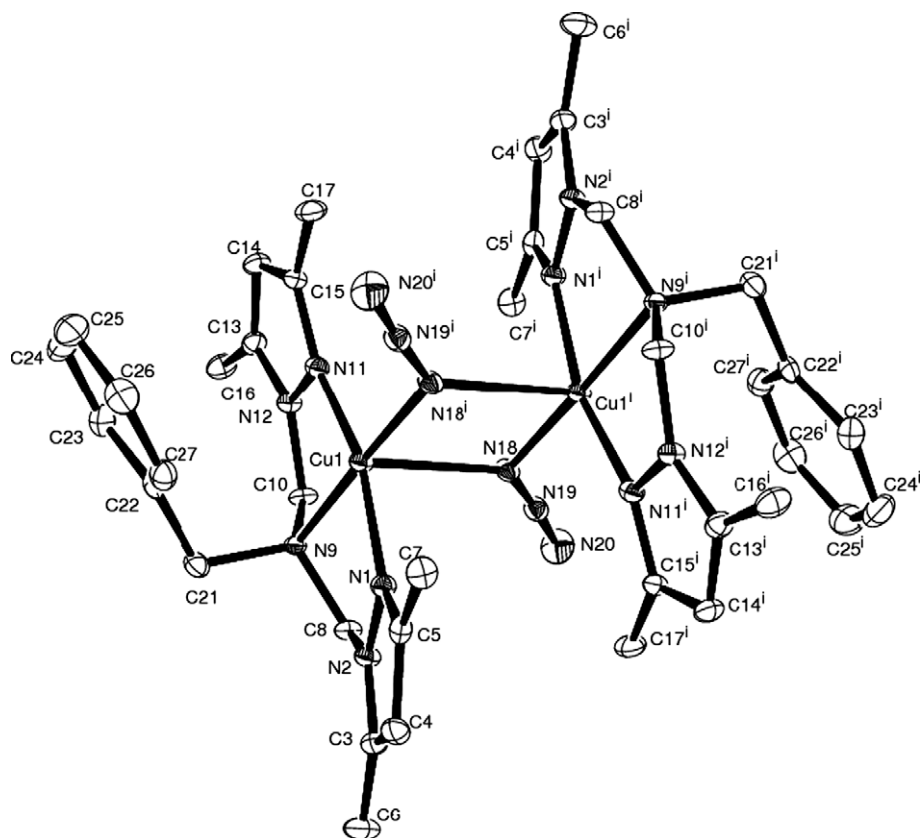


Fig. 1. The ORTEP diagram of complex **2** plotted at 30% probability.

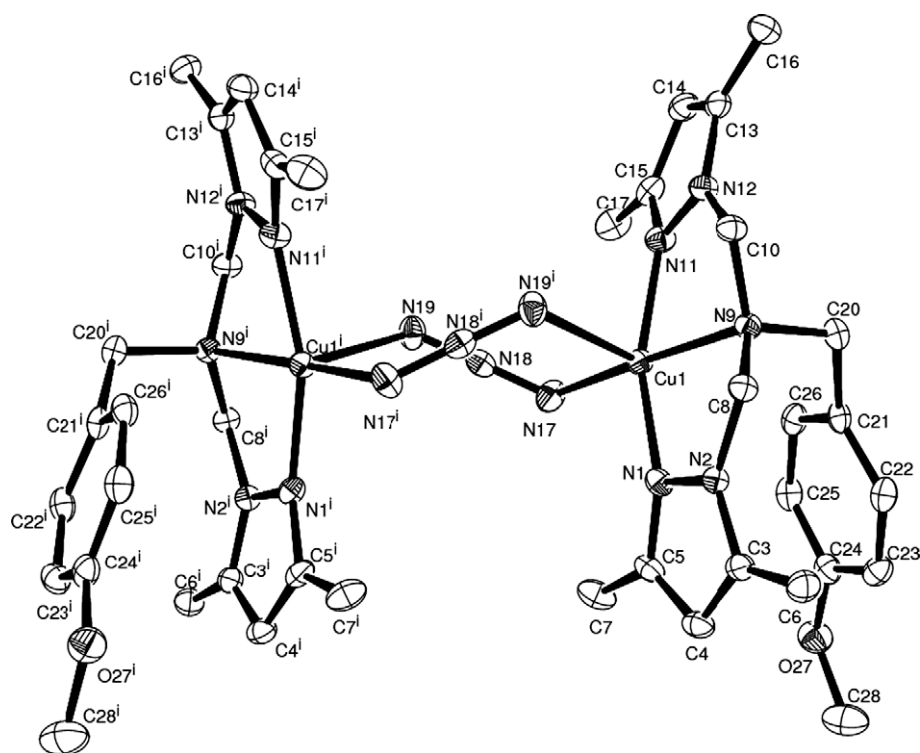


Fig. 2. The ORTEP diagram of complex **1** plotted at 30% probability.

gen atom of one of the bridging azide, Cu1–N18_a = 1.9619(17) occupy the equatorial plane. The axial position is occupied by the sec-

ond bridging azide group [Cu1–N18 = 2.4272(16) Å] at a rather longer distance. The two azide ions are related by crystallographic

center of inversion. The Cu1–N1 = 1.980(2) Å, Cu1–N9 = 2.080(16) Å, Cu1–N11 = 1.972(17) Å, and Cu1–N18_a = 1.962(17) Å distances are similar to those observed for related complexes of ligands with pyrazole and pyridine donor groups [50,51]. N–Cu–N bond angles vary from 81.04(6)° to 178.30(7)°. The two coordinated pyrazolyl nitrogens make a biting angle of N1–Cu1–N11 = 163.01(7)° with central metal ion. Similarly, the amino nitrogen (N9) and azide nitrogen (N18) make an angle of 178.30(7)°. Thus, the geometry around copper ion can be best described as a distorted square pyramid (**aSP**). The Cu···Cu distance is 3.287 Å. The linear azide ions related by the molecular inversion center are bridging the two copper centers through one nitrogen atom (**EO** mode). Each bridging nitrogen atom simultaneously occupies an equatorial position on Cu1 and an axial position on the other Cu1.

3.2. Structural description of $[\{Cu(L^{OMe})(\mu-1,3-N_3)\}_2(ClO_4)](2)$ (**EE**)

Compound **2** crystallizes from methanol as dark green solids. The details of crystal structural determination for the compound **2** reported here are given in Table 2. Selected bond distances and angles for compound **2** are given in Table 3. The ORTEP diagram of cationic part of **2** is given in Fig. 2. There are four dimeric units, $[CuL(\mu-1,3-N_3)]_2^{2+}$ in the unit cell, and two are isolated from other two by six perchlorate anions. The perchlorate ions are found to be normal though they are not coordinated to the metal ions. Within a dimeric unit, the copper(II) centers are symmetrically related (symmetry $-x + 1, y, -z + 3/2$) and are bridged by azide ions in an asymmetric **EE** fashion. As like **1** here also Cu(II) ion is coordinated to five nitrogens, three nitrogen atoms from two pyrazolyl and one amino nitrogen of L^{OMe} and a nitrogen atom of one of the bridging azide (Cu1–N17 = 1.9593(2) Å) lying in the equatorial plane. The axial position is occupied by the second bridging azide group at a rather longer distance (Cu1–N19_a = 2.403(2) Å). The Cu–N_{pyrazole} (Cu1–N1 = 1.9656(2) Å and Cu1–N11 = 1.974(2) Å) and Cu–N_{amine} (Cu1–N9 = 2.0755(2) Å) distances are similar to those observed for related complexes of ligands with pyrazole and pyridine donor groups [52]. N–Cu–N bond angles vary from 82.13(7)° to 174.6(8)°. The two coordinated pyrazolyl nitrogens make a biting angle of 161.2(7)° with central metal ion. Similarly, the amino nitrogen (N9) and azide nitrogen N17 and N19 make an angle of 174.6(8)° and 89.86(7)° respectively. Thus the geometry around copper ion can be best described as a distorted square pyramid. The Cu···Cu distance is 5.063 Å and comparable in the case of a similar compound [50,51]. It is noteworthy that in an analogous asymmetrically bridged aliphatic triamine ligand complex $Cu_2(\mu-N_3)_2(Me_5dien)_2(BPh_4)_2$ the Cu–Cu separation is only (5.2276(7) Å) [53]. The **EE** bridging azide is quasi-linear; the N17–N18–N19 bond angle is 177.71°. The Cu1_a–N19–N18 and Cu1–N17–N18 angles are 119.26(15)° and 120.32(16)° respectively, and the Cu1–(N₃)₂–Cu1_a unit forms a chair configuration. The N–N bond lengths for the bridging azide ligand are different from one another (N(6)–N(7) 1.181(6) Å and N(7)–N(8) 1.161(6) Å). The amine and pyrazole rings can be considered as practically planar.

3.3. Magnetic properties

As mentioned in the introduction, an unusual range of magnetic behavior (from ferro- to antiferro-) can be observed based on the nature of coordination of the azide bridging groups. In di-bridged complexes with one or more symmetric **EO** bridges, the interaction between the metal ions is strongly ferromagnetic [33]. On the other hand, with one or more symmetric **EE** azido bridges, the interaction is strongly antiferromagnetic [32,11]. In complexes with asymmetric **EE** azido bridge with short and long Cu–N_{azide}

bonds, the interaction is either negligible or very weakly antiferromagnetic, depending on the geometry which tends to be trigonal bipyramidal or Square Pyramidal, respectively [31].

3.3.1. Magnetic susceptibility of complex 1 (**EO**)

The two copper atoms are symmetrically equivalent and possess *aSP* (asymmetric Square Pyramidal) geometry. Complexes with asymmetric **EO** azido bridge are rare, and the interaction between metal centers is weak to moderately strong ferromagnetic [33]. Thus based on the earlier observations it is expected that complex **1** would provide moderate ferromagnetic interaction between two copper(II) paramagnetic centers.

Variable-temperature magnetic susceptibility measurements were performed on a polycrystalline sample in the range 2–300 K, and the results are shown in Fig. 3 in the form of μ_{eff}/μ_B and $M_{\text{mol}}/N_A\mu_B\mu_{\text{eff}}$ versus T plots. At room temperature, the μ_{eff} value is 2.14 μ_B , which is close to the spin-only value of 2.45 μ_B expected for two uncoupled $S = 1/2$ spin systems. As the temperature is lowered, the μ_{eff} value continuously increases and reaches a value of 3.32 μ_B at 5.00 K.

The magnetic data were successfully characterized with the spin Hamiltonian for a coupled dimer is (Eq. (1))

$$\hat{H} = -J(S_A \cdot S_B) + \mu_B B \cdot g \cdot (S_A + S_B) \quad (1)$$

where $|J|$ parameter characterizes the energy gap between the singlet ($S = 0$) and triplet state ($S = 1$) resulting from the coupling of two local spins $S_A = S_B = 1/2$. For the molar magnetization simple formula exists which is expressed as in Eq. (2):

$$M_{\text{mol}} = \mu_B g N_A [\exp((J+x)/kT) - \exp((J-x)/kT)] / [1 + \exp((J+x)/kT) + \exp(J/kT) + \exp((J-x)/kT)] \quad (2)$$

where $x = \mu_B g B$ [54,55]. The experimental data (both temperature and field dependent magnetization) were corrected to the underlying diamagnetism and fitted simultaneously by varying J and g parameters with fixed values of the temperature-independent paramagnetism term for two copper(II) centers as $\chi_{\text{TIP}} = +1.5 \text{ m}^3 \text{ mol}^{-1}$ (in SI units). The maximum on the susceptibility should be observed for antiferromagnetically coupled dimer and it holds $T_{\text{max}} = (J/k)/1.599$. By applying the best-fitted value, we are left with $T_{\text{max}}^{\text{Cal}} = 3.0 \text{ K}$, $J = -3.34 \text{ cm}^{-1}$, $g = 2.14$. The $T_{\text{max}}^{\text{Cal}}$ is in good agreement with the experimental value $T_{\text{max}}^{\text{Obs}} = 2.9 \text{ K}$ [54,55].

3.3.2. Magnetic susceptibility of complex 2 (**EE**)

The magnetic data were successfully characterized with the spin Hamiltonian for coupled dimer as in Eq. (1) where $|J|$ parameter characterizes the energy gap between the singlet ($S = 0$) and triplet state ($S = 1$) resulting from the coupling of two local spins $S_A = S_B = 1/2$. For the molar magnetization Eq. (2) exists.

The experimental data (both temperature and field dependent magnetization) were corrected to the underlying diamagnetism and fitted simultaneously by varying J and g parameters with fixed values of the temperature-independent paramagnetism term for two Cu(II) centers as $\chi_{\text{TIP}} = +1.5 \text{ m}^3 \text{ mol}^{-1}$ (in SI units) (Fig. 4). Fig. 5 shows alternative fit with the molecular-field correction with spin Hamiltonian by Eq. (3):

$$\hat{H} = -J(S_A \cdot S_B) + \mu_B B \cdot g \cdot (S_A + S_B) - zj \langle S_z \rangle S_z \quad (3)$$

where zj is the common molecular-field parameter which is due to small intermolecular interactions and S_z is a thermal average of the spin [56]. There is no visible change in parameters ($J = +19.7 \text{ cm}^{-1}$, $g = 2.17$, Eq. (2)) on considering the small intermolecular interactions ($J = +19.9 \text{ cm}^{-1}$, $g = 2.16$ and $zj = +0.025 \text{ cm}^{-1}$, Eq. (3)) indicating negligible intermolecular interactions and this is supported by the wide separation (8.279 Å) between the two nearest copper(II) centers of two separate dimers.

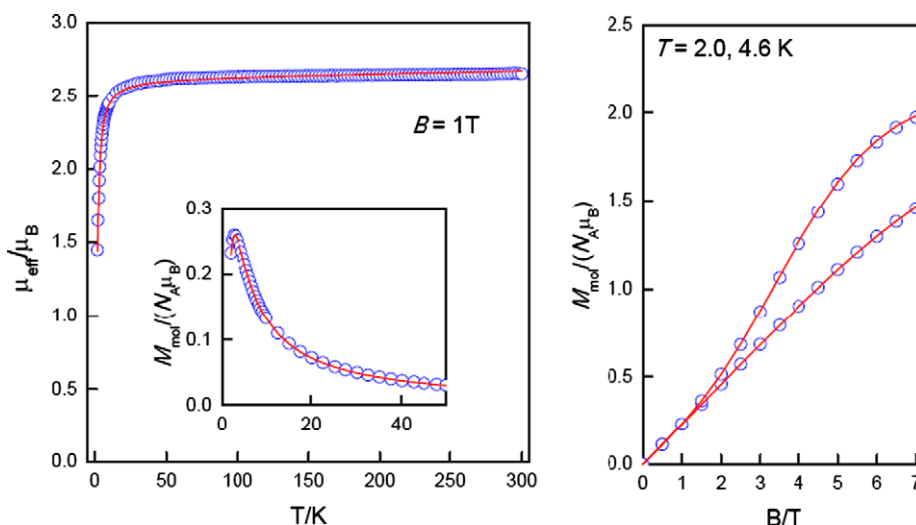


Fig. 3. Left: temperature dependence of the effective magnetic moment of complex **1** (EO) (calculated from magnetization at $B = 1.0$ T) with the low-temperature region expanded in the inset; right: field-dependence of magnetization at $T = 2.0$ and 4.6 K. circles – experimental points, lines – calculated using the best-fit parameters: $J = -3.34$ cm $^{-1}$, $g = 2.14$.

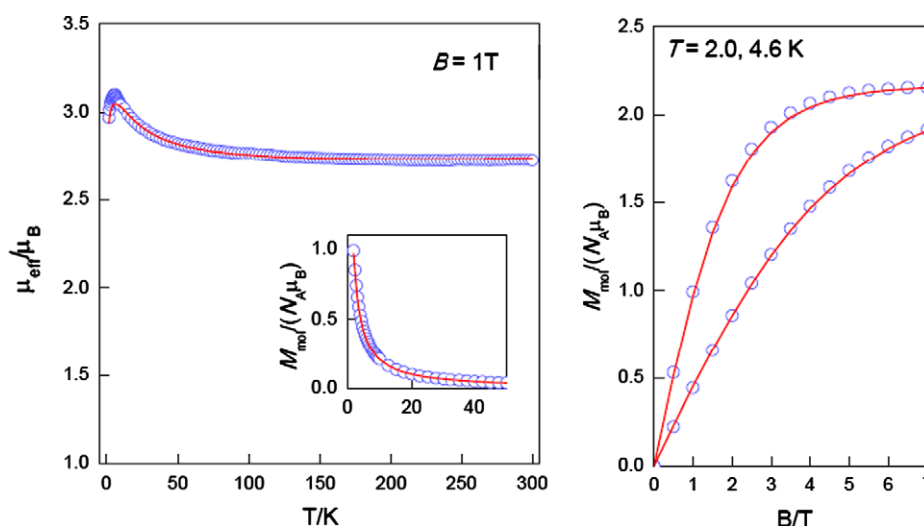


Fig. 4. Left: temperature dependence of the effective magnetic moment of complex **2** (EE) (calculated from magnetization at $B = 1.0$ T) with the low-temperature region expanded in the inset; right: field-dependence of magnetization at $T = 2$ and 4.6 K. circles – experimental points, lines – calculated using the best-fit parameters: $J = +19.7$ cm $^{-1}$, $g = 2.17$.

3.4. Electronic spectra

The UV spectra of the complexes **1–4** in MeCN are very similar (Fig. 6). The electronic spectra show bands in the range of wavelength 393–414 nm with molar extinction coefficients values, $\epsilon = 2692, 4860, 4880$ and 2516 dm 3 mol $^{-1}$ cm $^{-1}$ for X = Cl, H, Me and OMe, respectively and arise mainly due to the pyrazole nitrogen to metal charge transfer transition (LMCT).

3.5. Cyclic voltammetric studies

Electrochemical measurements were carried out using a computer-controlled AUTOLAB (model 263A VERSASTAT) electrochemical instrument with Pt-tip as working electrode. Cyclic voltammograms were recorded at 25 °C versus Ag/AgCl electrode in MeCN under pure N $_2$ atmosphere with 0.1 M tetrabutylammonium perchlorate (TBAPC) as supporting electrolyte. The cyclic vol-

tammetric studies on the metal centers showed quasi-reversible waves (Fig. 7) and represented in Eq. (4)



Details of $E_{1/2}$ values are shown in Table 4. An attempt was taken to correlate the $E_{1/2}$ values for the two processes with substituent constants (σ).

The plots of $E_{1/2}$ of the dinuclear copper(II) complexes versus σ of pyrazole-based tripodal ligands bearing different substituents on the *para*-position of benzene ring seem to be interesting to understand the effect of substituents on $E_{1/2}$ and to elucidate the reduction mechanism. Many electrochemical processes have been shown to correlate quite well with Hammett substituent constants [57]. It is not surprising that the electrochemical processes which involve addition or removal of electrons from an organic framework should correlate with the ability of substituents to withdraw or supply electron density to that framework.

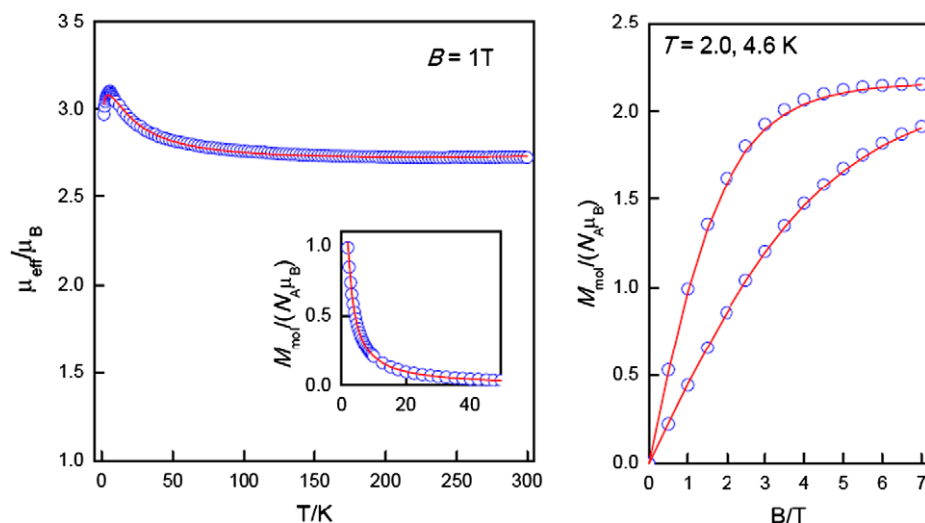


Fig. 5. Left: temperature dependence of the effective magnetic moment of complex **2** (EE) (calculated from magnetization at $B = 1$ T) with the low-temperature region expanded in the inset; right: field-dependence of magnetization at $T = 2$ and 4.6 K. circles – experimental points, lines – calculated using the best-fit parameters: $J = +19.9$ cm $^{-1}$, $g = 2.16$ and $zJ = +0.025$ cm $^{-1}$.

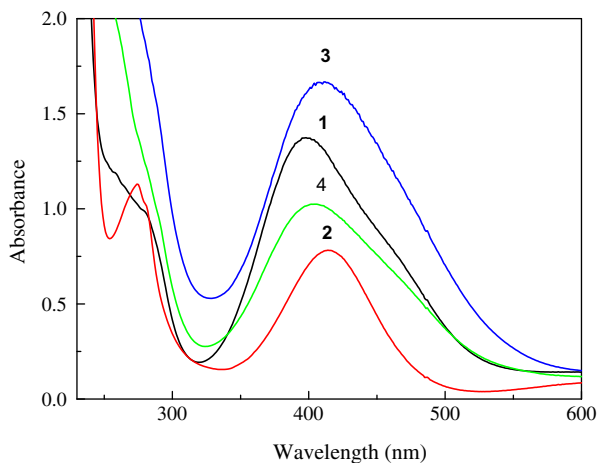


Fig. 6. Electronic spectra of complexes **1** (H), **2** (OMe), **3** (Me) and **4** (Cl) in MeCN, $[C] = 5.0 \times 10^{-4}$ M.

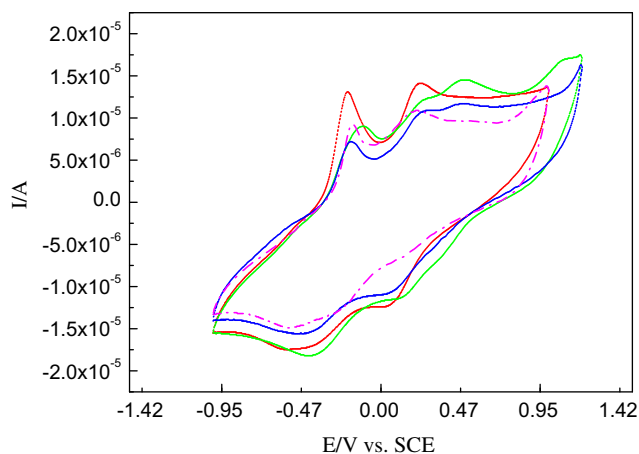


Fig. 7. Cyclic voltammograms of **1–4** in MeCN under N_2 atmosphere in MeCN using a Pt-tip as working electrode and TBAP (0.10 M) as supporting electrolyte at 50 mV s $^{-1}$ scan rate vs. Ag/AgCl. $[[Cu(L^H)N_3]_2(ClO_4)_2]$ (**1**) (colour), $[[Cu(L^{OMe})N_3]_2(ClO_4)_2]$ (**2**) (colour), $[[Cu(L^{Me})N_3]_2(ClO_4)_2]$ (**3**) (colour), $[[Cu(L^{Cl})N_3]_2(ClO_4)_2]$ (**4**) (colour).

Table 4

Summary of electrochemical studies of complexes **1–4** in MeCN under nitrogen atmosphere with $[C] = 1.0 \times 10^{-3}$ M, TBAP = 0.10 M as supporting electrolyte.

Compounds	E_{pa}	E_{pc}	$E_{1/2}$	E_{pa}	E_{pc}	$E_{1/2}$
1 (L^H)	−0.198	−0.436	−0.317	0.233	0.046	0.140
2 (L^{OMe})	−0.107	−0.399	−0.253	0.486	0.125	0.306
3 (L^{Me})	−0.180	−0.435	−0.308	0.261	0.060	0.161
4 (L^{Cl})	−0.170	−0.535	−0.353	0.200	−0.254	−0.027

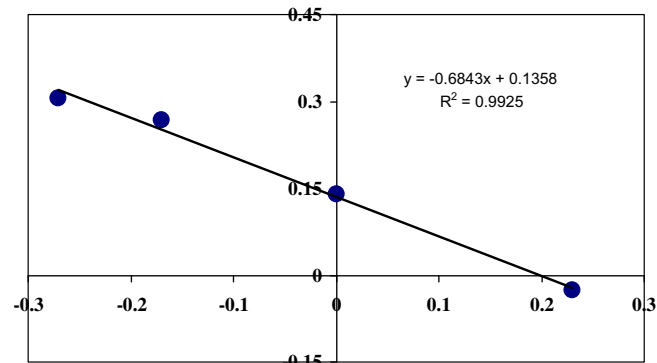


Fig. 8. Hammett plot of $E_{1/2}$ vs. σ and ρ (for the $Cu^{II}Cu^{III}-Cu^{III}Cu^{III}$ couple. Conditions are same as mentioned in Fig. 7).

A reasonable linear relation was observed when we plot $E_{1/2}$ (for $Cu^{II}Cu^{II}-Cu^{II}Cu^{III}$ and $Cu^{II}Cu^{III}-Cu^{III}Cu^{III}$ oxidation) versus σ and ρ values obtained from the slopes are -0.182 ($R^2 = 0.92$) and -0.684 ($R^2 = 0.99$) (Fig. 8) respectively. The strong dependence of $E_{1/2}$ on the substituent constants for the latter reaction compared to the former is due to the fact that electron withdrawing substituents destabilize the higher oxidation states more prominently than lower one. This also explains the observation of negative ρ values for these processes.

4. Conclusion

Four azido-bridged dinuclear copper(II) complexes of N-methyl pyrazole-based tripodal ligands, L^X , $[X = H$ (**1**), OMe (**2**), Me (**3**) and

Cl (4)] have been synthesized. Complexes **1** and **2** have been characterized structurally and cryo-magnetic studies were performed on them. In Complex **1** the two bridging azide ligands connect the two metal centers by **EO** fashion with α SP geometry and showed very weak antiferromagnetic interactions ($J = -3.34 \text{ cm}^{-1}$). On the contrary, in complex **2**, an **EE** bridging was observed and exhibits moderately strong ferromagnetic interaction ($J = +19.7 \text{ cm}^{-1}$). Cyclic voltammetric studies were performed on all the four complexes and $E_{1/2}$ for $\text{Cu}^{\text{II}}\text{Cu}^{\text{I}} \rightarrow \text{Cu}^{\text{II}}\text{Cu}^{\text{III}}$ and $\text{Cu}^{\text{II}}\text{Cu}^{\text{III}} \rightarrow \text{Cu}^{\text{III}}\text{Cu}^{\text{III}}$ oxidations were plotted against σ (substituent constants) and nice correlations were found with $\rho = -0.182$ ($R^2 = 0.92$) and -0.684 ($R^2 = 0.99$) (Fig 6) respectively.

Supplementary data

CCDC 716781 and 716782 contain the supplementary crystallographic data for complexes **1** and **2**. These data can be obtained free of charge via <http://www.ccdc.cam.ac.uk/conts/retrieving.html>, or from the Cambridge Crystallographic Data Centre, 12 Union Road, Cambridge CB2 1EZ, UK; fax: (+44) 1223-336-033; or e-mail: deposit@ccdc.cam.ac.uk.

Acknowledgements

Financial supports from DRDO (Ref. ERIP/ER/0503510/M/904) and DST (Ref. SR/S1/IC-35/2006), New Delhi, India are gratefully acknowledged. JM (MSM0021622415) and RH (MSM619 8959218) acknowledge the grants from the Ministry of Education, Youth and Sports of the Czech Republic.

References

- [1] H. Sigel, *Metal Ions in Biological Systems*, Dekker, New York, 1981.
- [2] K.D. Karlin, Z. Tyelkar, *Bioinorganic Chemistry of Copper*, Kluwer, New York, 1993.
- [3] T. Tsukihara, H. Aoyama, E. Yamashita, T. Tomizaki, H. Yamaguchi, K. Shinzawa-Itoh, R. Nakashima, R. Yaono, S. Yoshikawa, *Science* 269 (1995) 1069.
- [4] S. Iwata, C. Ostermaier, B. Ludwig, H. Michel, *Nature* 376 (1995) 660.
- [5] P.M.H. Kronek, W.A. Antholine, J. Riester, W.G. Zumft, *FEBS Lett.* 242 (1988) 70.
- [6] I.A. Koval, P.J. Gamez, Reedijk, *Mimicking Nature: Bio-Inspired Models of Copper Proteins*, in: Professor Bruno Pignataro (Eds.), *Tomorrow's Chemistry Today*, Copyright © 2008, Wiley-VCH Verlag GmbH & Co. KGaA (Chapter).
- [7] J.H. Rodriguez, J.K. Mc Cusker, *J. Chem. Phys.* 116 (2002) 6253.
- [8] E. Ruiz, S. Alvarez, *Chem. Phys. Chem.* 6 (2005) 1094.
- [9] E. Ruiz, A. Rodriguez-Fortea, J. Tercero, T. Cauchy, *J. Chem. Phys.* 123 (2005) 74102.
- [10] M.W. Göbel, *Angew. Chem., Int. Ed.* 33 (2008) 1411.
- [11] V. Mckee, M. Zvagulis, J.V. Dagdigian, M.G. Patch, C.A. Reed, *J. Am. Chem. Soc.* 106 (1984) 4765.
- [12] O. Kahn, *Molecular-Magnetism*, VCH, New York, 1993.
- [13] O. Kahn, in: R.D. Willett, D. Gatteschi, O. Kahn (Eds.), *Magneto-Structural Correlations in Exchange Coupled Systems*, D. Reidel, Dordrecht, The Netherlands, 1985.
- [14] O. Kahn, S. Sikorav, J. Gouteron, S. Jeannin, Y. Jeannin, *Inorg. Chem.* 22 (1983) 2877.
- [15] M.A.M. Abu-Youssef, M. Drillon, A. Escuer, M.A.S. Goher, F.A. Mautner, R. Vicente, *Inorg. Chem.* 39 (2000) 5022.
- [16] M. Monfort, I. Resino, J. Ribas, H. Stoeckli-Evans, *Angew. Chem., Int. Ed.* 39 (2000) 191.
- [17] Zhi-Xin Miao, Ming-Xing Li, Min Shao, Hong-Jiang Liu, *Inorg. Chem. Commun.* 10 (2007) 1117.
- [18] Fu-Chen Liu, Jie Ouyang, *Acta Crystallogr., Sect. E: Struct. Rep. Online* 64 (2008) m6.
- [19] F.-C. Liu, Yong-Fei Zeng, Jiong-Peng Zhao, Bo-Wen Hu, Xian-He Bu, J. Ribas, S.R. Batten, *Inorg. Chem. Commun.* 10 (2007) 129.
- [20] Yong-Fei Zeng, Fu-Chen Liu, Jiong-Peng Zhao, Shuang Cai, Xian-He Bu, Joan Ribas, *Chem. Commun.* (2006) 2227.
- [21] Qiao-Fang Yang, Zhi-Guo Gu, Cheng-Hui Li, Jian-Qing Tao, Jing-Lin Zuo, Xiao-Zeng You, *Inorg. Chim. Acta* 360 (2007) 2875.
- [22] A. Escuer, M. Font-Bardia, S.S. Massoud, F.A. Mautner, E. Penalba, X. Solans, R. Vicente, *New J. Chem.* 28 (2004) 681.
- [23] G. Ambrosi, P. Dapporto, M. Formica, V. Fusi, L. Giorgi, A. Guerri, P. Paoli, R. Pontellini, P. Rossi, *Dalton Trans.* (2004) 3468.
- [24] K. Dhara, S. Karan, J. Ratha, P. Roy, G. Chandra, M. Manassero, B. Mallik, P. Banerjee, *Chem. Asian J.* 2 (2007) 1091.
- [25] D.-Y. Wu, W. ei Huang, W.-J. Hua, Y. Song, C.-Y. Duan, S.-H. Li, Q.-J. Meng, *Dalton Trans.* (2007) 1838.
- [26] S. Chattopadhyay, M.S. Ray, M.G.B. Drew, C. Diaz, A. Figuerola, C. Diaz, A. Ghosh, *Polyhedron* 25 (2006) 2241.
- [27] Sk.H. Rahaman, D. Bose, R. Ghosh, G. Mostafa, H.-K. Fun, B.K. Ghosh, *Struct. Chem.* 18 (2007) 237.
- [28] Z.-. You, P. Zhou, *Transit. Met. Chem.* 33 (2008) 453.
- [29] A. Escuer, R. Vicente, M.A.S. Goher, F.A. Mautner, *Inorg. Chem.* 36 (1997) 3440.
- [30] F.A. Mautner, R.R. Cortés, L. Lezama, T. Rojo, *Angew. Chem., Int. Ed.* 35 (1996) 78.
- [31] V. Mckee, J.V. Dagdigian, R. Bau, C.A. Reed, *J. Am. Chem. Soc.* 103 (1981) 7000.
- [32] Y. Agnus, R. Lewis, J.P. Gisselbrecht, R. Weiss, *J. Am. Chem. Soc.* 106 (1984) 93.
- [33] R. Cortes, M.K. Urtiga, L. Lezama, J.S.R. Larramandi, M.I. Arriortua, T. Rojo, *J. Chem. Soc., Dalton Trans.* (1993) 3685.
- [34] E. Ruiz, J. Cano, S. Alvarez, P. Alemany, *J. Am. Chem. Soc.* 120 (1998) 11122.
- [35] K.D. Karlin, Z. Tyelkar (Eds.), *Bioinorganic Chemistry of Copper*, Chapman and Hall, New York, 1993.
- [36] E.I. Solmon, U.M. Sundaram, T.E. Machonkin, *Chem. Rev.* 96 (1996) 2563.
- [37] M. El Kodadi, M. Fouad, A. Ramdani, D. Eddike, M. Tillard, C. Belin, *Acta Crystallogr., Sect. E: Struct. Rep. Online* 60 (2004) m426.
- [38] H.L. Blonk, W.L. Driessen, J. Reedijk, *J. Chem. Soc., Dalton Trans.* (1985) 1699.
- [39] G.J. Kleywegt, W.G.R. Wiesmeijer, G.J. Van Driel, W.L. Driessen, J. Reedijk, J.H. Noordik, *J. Chem. Soc., Dalton Trans.* (1985) 2177.
- [40] M. El Kodadi, F. Malek, R. Touzani, A. Ramdani, S. El Kadiri, D. Eddike, *Molecules* 8 (2003) 780.
- [41] A. Ramdani, M. El Kodadi, M. Fouad, D. Eddike, M. Tillard, C. Belin, *Acta Crystallogr., Sect. E: Struct. Rep. Online* 61 (2005) m346.
- [42] Z.-H. Zhang, Z.-H. Ma, Y. Tang, W.-J. Ruan, *J. Chem. Cryst.* 34 (2004) 119.
- [43] W.L. Driessen, H.L. Blonk, W. Hinrichs, J. Reedijk, *Acta Crystallogr., Sect. C: Cryst. Struct. Commun.* 43 (1987) 1885.
- [44] P.D.W. Boyd, A.K. Burrell, C.E.F. Rickard, *Acta Crystallogr., Sect. C: Cryst. Struct. Commun.*, 53 (1997) 1549.
- [45] Y.C.M. Pennings, W.L. Driessen, J. Reedijk, *Acta Crystallogr., Sect. C: Cryst. Struct. Commun.* 44 (1988) 2095.
- [46] Z. Chen, N. Karasek, D.C. Craig, S.B. Colbran, *J. Chem. Soc., Dalton Trans.* (2000) 3445.
- [47] S. Bhattacharyya, S.B. Kumar, S.K. Dutta, E.R.T. Tiekink, M. Chaudhury, *Inorg. Chem.* 35 (1996) 1967.
- [48] M.R. Malachowski, M.G. Davidson, *Inorg. Chim. Acta* 162 (1989) 199.
- [49] G.M. Sheldrick, *Acta Cryst.* A64 (2008) 112.
- [50] I.B. Waksman, M.L. Boillot, O. Kahn, S. Sikorov, *Inorg. Chem.* 23 (1984) 4454.
- [51] A.A. Watson, D.A. House, P.L. Steel, *Inorg. Chim. Acta* 130 (1987) 167.
- [52] P. Manikandan, R. Muthukumar, K.R. Justin Thomas, B. Varghese, G.V.R. Chandramauli, P.T. Manoharan, *Inorg. Chem.* 40 (2001) 2378.
- [53] P. Chadhuri, K. Oder, K. Weighardt, B. Nuber, J. Weiss, *Inorg. Chem.* 25 (1986) 2818.
- [54] T.R. Felthouse, D.N. Hendrickson, *Inorg. Chem.* 17 (1978) 444.
- [55] R. Boca, *Theoretical Foundation of Molecular Magnetism*, Elsevier, Amsterdam, 1999.
- [56] C.J. O'Connor, *Prog. Inorg. Chem.* 29 (1982) 203.
- [57] A. Endo, *Bull. Chem. Soc. Jpn.* 56 (1983) 2733.